Carbon Capture and Utilization by Mineral Carbonation with CKD in Aqueous Phase: Experimental Stage and Characterization of Carbonated Products

PEDRAZA, J.I. [a*]; SUAREZ, L.A.[a,c]; MARTINEZ, L. A.[a]; ROJAS, N.Y. [a]; TOBÓN, J.I. [b]; RAMIREZ, J.H. [a]; ZEA, H.R.[a]; CÁCERES, A. A.[c]

a. Departamento de Ingeniería Química y Ambiental. Facultad de Ingeniería. Universidad Nacional de Colombia. Bogotá, Colombia.
b. Departamento de Materiales y Minerales. Facultad de Minas. Universidad Nacional de Colombia. Medellín, Colombia.
c. Programa de Ingeniería Ambiental. Universidad ECCI. Bogotá, Colombia
** Corresponding author, jipedrazav@unal.edu.co*

Abstract

Carbon dioxide capture and reuse techniques are being developed to reduce greenhouse gas (GHG) emissions from the industrial sector at the same time that high added value by-products are obtained. Carbon capture by mineral carbonation of CO_2 using industrial waste is an interesting technology. Its rate and effectiveness depends on four main parameters: sample water content (or amount of mixed water or liquid / solid ratio); particle size; temperature, and pressure. Cement kiln dust, which is a residue of the cement industry, could be considered the most suitable material for this purpose, with a high calcium and magnesium content. We used a response-surface experimental design model to assess CO_2 carbonation mineral techniques and determine its uptake potential, and the products' physical-chemical and mineralogical properties. Diffractogram showed that a carbonated phase was formed after the reaction, increasing amount of calcium and magnesium carbonates. Theoretical uptake was calculated as 23.4 % w/t, instead, experimental yield was found out between 7-22% compared to the theoretically amount of CO_2 sequestration.

Keywords: *carbon capture and utilization, cement kiln dust, industrial waste, mineral carbonation.*

1. Introduction

Carbon dioxide capture and reuse techniques are being developed to reduce greenhouse gas (GHG) emissions from the industrial sector at the same time that high added value by-products are obtained. Several types of industrial wastes have high content of cations (eg Ca, Mg, Al and Fe in the form of reactive oxides and hydroxides), which make them especially attractive for their utilization by mineral carbonation process. In this process, it is possible to use industrial waste from industries such as: cement manufacturing, municipal and clinical waste incineration, electric power generation, steel manufacturing, ceramics, aluminum manufacturing and paper mills (Styring et al., 2014). Nowadays, world cement production is around of 4.2 Gt, and contributes to 5-8% of global CO_2 emissions (Huntzinger et al, 2009)(Bobicki et al, 2012). Cement industry produces around 0.85-1.0 t CO_2/t Clinker (Bernal & Saavedra, 2008), in addition, this industry produces 0.15-0.3 t alkaline waste/t Clinker annually (Sanna, 2015). Cement Kiln Dust (CKD), which is a clinker production sub-product, contains around of 35% w/w calcium oxide –CaO- and 2% w/w of magnesium oxide – MgO, and has a

uptake potential among 191-256 kg CO_2/t CKD, which is equivalent to 43-58 kg CO_2/t Clinker (Styring et al., 2014). CKD production is around 0.15-0.20 t per ton of cement. (Sanna, 2015)

Carbon Capture is considered as a carbon mitigation strategy for the industrial and power generation sectors. It includes two categories: carbon capture and storage (CCS), and carbon capture and use (CCU) (Roh, Lee, & Gani, 2016). CCS is a process consisting of separating CO_2 emitted by industry power generation facilities, transporting it to a storage place and isolating it from the long-term atmosphere. In the case of CCU, it involves the conversion of captured CO_2 into usable materials, either as a final product, or as raw material into a production process.

Studying mineral carbonation of CO_2 using industrial waste in Colombia can provide useful information for a number of companies that will contribute to reducing emissions within the framework of Colombia's GHG emission reduction commitments in international conventions such as COP 21 (IDEAM, 2015). National mitigation actions focus on reducing of deforestation and degradation, using lower carbon intensity fuels, energy efficiency, solid waste management, sustainable production and carbon reductions of the cement, steel, pulp of paper and cardboard industries, and promoting the capture, storage and use of CO_2 from hydrocarbon production, transportation and refining activities. However, the transformation of captured CO_2 into products with high added value has not yet been considered within the national policies (IDEAM, 2015). This technique is outlined with a great potential for development, especially in the industrial sector, with an emission of 11% of the total country, equivalent to 16.6 Mt CO_2 / year (IDEAM, 2015).

Mineral carbonation includes chemical reactions to obtain synthetic carbonates expressed in Eq. 1, where Me means a divalent metal (Fernández Bertos et al, 2004):

$$MeO + CO_2 \leftrightarrow MeCO_3 + heat \quad (1)$$

Carbonation uptake of a waste is determined by the reactivity of its alkaline components, the kinetics of the reaction and the reaction conditions (Kirchofert et al, 2013). In aqueous phase, alkaline waste is first solvated in water and then, comes into contact with CO_2. (Ukwattage et al, 2017). In this route, water plays a catalytic role because it facilitates the conversion of dissolved CO_2 into carbonated species through the previous formation of carbonic acid (Eq. 2 - 4), (Yuen et al, 2016). Also, the carbonation reaction is regulated by the equilibrium of the solution: As the calcium ions are converted to calcium carbonate and precipitate, more calcium hydroxide dissolves to equalize the concentration of calcium ions (Ca^{2+}), (Eq. 5 - 6).

$$CO_{2\,(g)} \rightarrow CO_{2\,(ac)} \quad (2)$$

$$H_20 + CO_{2\,(ac)} \rightarrow H_2CO_{3\,(ac)} \quad (3)$$

$$H_2CO_{3\,(ac)} \rightarrow H^+_{(ac)} + HCO_3^- \rightarrow 2H^+_{(ac)} + CO_3^{-2} \quad (4)$$

$$CaO + H_2O \rightarrow Ca(OH)_2 \rightarrow Ca^{+2}_{ac} + 2OH^- \quad (5)$$

$$Ca^{+2}_{ac} + CO_3^{-2} \rightarrow CaCO_{3(s)} \quad (6)$$

We aimed to study the carbonation process yield at the laboratory scale in order to determine the performance of CO_2 capture by mineral carbonation of CKD in aqueous phase. First, we estimated the theoretical uptake from CKD composition. Second, we carried out groups of experiments in a laboratory-scale reactor. The obtained products were characterized using different analytical techniques to determine the experimental yield, and identify the mineralogical transformation and crystallographic phases present in the products.

2. Materials and methods

2.1 Material selection

The cement industry produces alkaline solid waste with presence of ions **(**Ca^{+2}, Mg^{+2}). CKD is a fine-grained, solid and highly alkaline particle material composed especially of oxidized, anhydrous and micrometric particles collected during the production of Cement Clinker (Kunal et al, 2012). The CKD tested here was a dry sample collected directly from one of the cyclones of a local cement plant in Colombia.

2.2 Mineral carbonation test in laboratory scale

The reactivity of a capture material depends on its calcium and magnesium content. The theoretical uptake potential is based on the metallic oxides content. According to the empirical equation (7), CO_2 consumed is equivalent to the difference between the mass consumed in the chemical reaction and the initial waste mass (El-Naas et al, 2015), (Huntzinger et al, 2009).

$$\%CO_2 = 0{,}785(\%CaO - 0{,}56\%CaCO_3 - 0{,}7\%SO_3) + 1{,}091\%MgO + 0{,}71\%Na_2O + 0{,}468\%K_2\,O \quad (7)$$

Experiments were carried out in a 700 mL batch reactor (Fig. 1), equipped with a thermocouple and a manometer. The CO_2 used was grade 4 Linde®. Water for the reaction media was distilled and deionized. Reaction time was set at 4 hours, and the stirring remained constant at 60 rpm. To establish the total number of experiments, we applied a *Response surface model*, using three levels for each factor: temperature between 30 – 70 °C, pressure between 4-12 bar, and molar ratio between 4-5 L/S (liquid/solid). We performed analysis of response-surface regression and multivariate statistical analysis (principal components analysis - PCA) to know the influence of pressure, temperature and molar relation on capture efficiency, using a trial version of Minitab® software.

For every batch, the reactor was loaded, sealed and purged with carbon dioxide. The aqueous phase (CKD and water) was stirred, and heated during the reaction time. Pressure was controlled and regulated by injecting more carbon dioxide if pressure decreased. After the reaction time, the remaining unreacted CO_2 was released, and carbonated products were extracted from the reactor, filtered and dried at 105 °C. In addition, these experiments were conducted under similar conditions (pressure and temperature) in water without CKD to determine the pressure drop caused solely by CO_2 solvation in water.

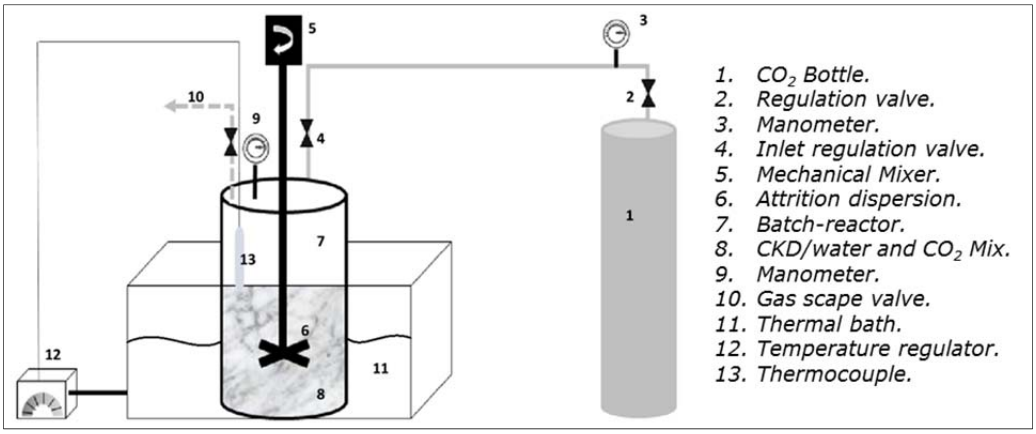

Fig. 1 Experimental set up.

According to corresponding states principle, when reduced pressure, P_r, is lower than 0.05, the ideal gas model can be used with an error lower than 5%. In this work, reduced pressure for CO_2 is 0.05-0.2 for the 4-12 bar interval, (critical pressure, $P_{c,\ CO2}$ = 73,98 bar). To obtain the mass (or the molar number of CO_2) consumed in reaction, the Redlich-Kwong model was used to determine the compressibility factor, z, considering the deviation of the properties of CO_2 from an ideal gas (Sun et al, 2012) (Gil Chaves et al, 2016).

2.3 Characterization of materials

Pre-carbonated and post-carbonated samples were characterized using analytical techniques. Chemical composition was determined using: i) X-Ray fluorescence (XRF) in a Magic Pro PW Philips WDX equipped with Rhodium Tube, where X-Ray irradiated the sample in turn emits spectrum of wavelength characteristic of type of elements present; and ii) Fourier Transform Infrared Spectroscopy FTIR BRUKER, where infrared light is applied to know the absorption spectrum of a solid or liquid.

Phase identification was determined by XRD, using a PANALYTICAL Model Xpert Pro range 5°-90° equipped with a copper tube; sample analysis was done using Xpert Highscore® 3.0 software; also, *Rielveld refinement* was performed in the FullProf® software in order to know amount of each phase. Morphological analysis was done using a Scanning Electron Microscope SEM, PHENOM PRO X, that produce of a sample by scanning the surface with Ray-X. In order to know the carbonate composition was used thermogravimetric analysis -TGA (using Mettler Toledo TGA) in nitrogen atmosphere. The particle size was determinate with a Mastersizer 3000 laser technique.

3. Results and discussion

3.1 CKD Characterization

CKD was sieved and the fraction around 40 µm was chosen for the experiment, considering that fine materials generally show higher carbonation efficiency because of their greater surface area (Fernández Bertos et al., 2004). According to chemical composition results, CKD contains a high amount of CaO and SiO_2. Percentages are concurrent with previous studies (Kunal et al 2012), Table 1.

Table .1 Elemental composition of CKD by XRF, wt %

Chemical compound	CKD tested	*CKD REFERENCE VALUE*	
		(Sreekrishnavilasam et al, 2006)	(Maslehuddin et al, 2009)
CaO	47.98	43.99	49.3
SiO_2	8.51	15.05	17.1
AlO_3	4.55	6.75	4.24
Fe_2O_3	2.81	2.23	2.89
MgO	0.61	1.64	1.14
P_2O_5	0.30	-	-
Na_2O	0.22	0.69	3.84
TiO_2	0.22	-	-
LOI	33	21.57	15.8

Fig. 2 shows that frequency bands of $CO_3^{2-}$are present in 1400 cm^{-1}, 873 cm^{-1}, characteristics of CKD (Martínez et al, 2014). Fig. 3 shows TG Analysis for CKD. Mass loss stars at 474°C. About 35.13% of the mass is lost around 740 °C, corresponding to the de-carbonation of $CaCO_3$ present in the sample into calcium oxide (CaO) and carbon dioxide (CO_2). Total amount of initial $CaCO_3$ in CKD was 9.97 mg.

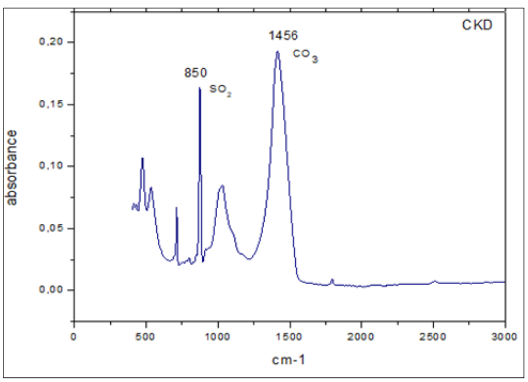

Fig. 2 FT-IR spectrogram for CKD

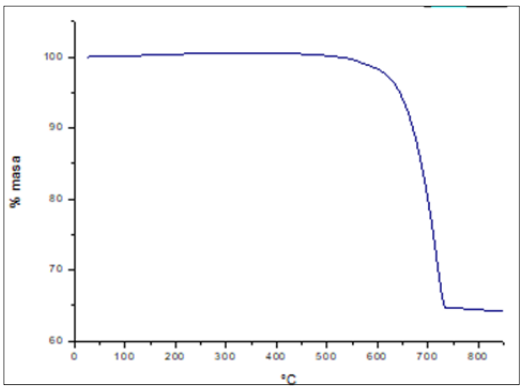

Fig. 3. TGA results for CKD (28,396 mg sample, nitrogen atmosphere)

Main phases identified by XRD were Calcium Oxide (CaO), Wollastonite (CaSiO), Portlandite ($Ca(OH)_2$), Quartz low (SiO_2), Fig. 3-a. Micrograph analysis shows fine and irregular particles that is characteristic of CKD (Ahmari & Zhang, 2013), Fig. 4-b.

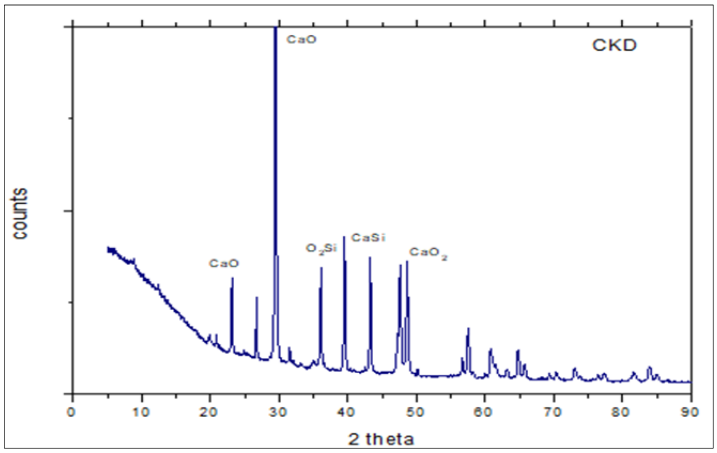

4-a. XRD analysis for CKD

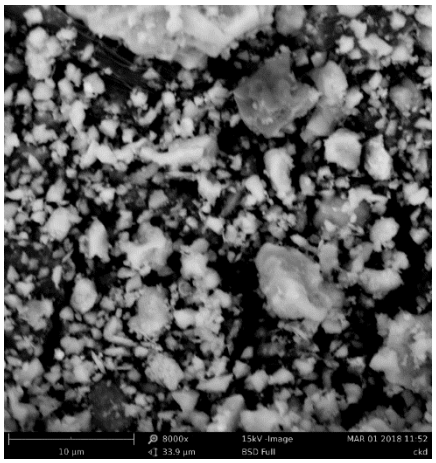

4-b. SEM analysis for CKD

Fig. 4. Morphological analysis for CKD (pre-carbonated sample)

3.2 Effect of temperature, pressure and molar ratio in CO_2 uptake yield

According to equation (7), the theoretical CO_2 uptake for CKD is 23.4 % w/t. It means that under ideal conditions, it is possible to capture 234 kg of CO_2 per ton of CKD. Experimental yield for mineral carbonation was calculated as CO_2 consumed in reaction measured by pressure drop, which is expressed in terms of the mass of CO_2 versus mass initial of CKD. It is between 7-22% for experimental values of pressure, temperature and ratio molar. Previous study for CKD, found an experimental uptake between 11-34% under ambient pressure and temperature in a column laboratory-scale (Huntzinger et al., 2009).

In this work, we evaluated the significance in the differences of the response variable (CO_2 capture) resulting from different treatment conditions. We examined the results of an analysis of for the response surface regression, setting a statistical confidence level of 95% ($\alpha = 0.05$). Results indicated that only pressure is significant on CO_2 capture (p-value = 0.008).

The Pareto diagram in Fig 5 shows that only pressure (A-factor) has strong predominance on response, whereas temperature and molar ratio have a weak influence on it. On other hand, Fig. 6 and Fig. 7 show, that increasing temperature decreases efficiency, because the solubility of CO_2 in the aqueous phase, according to Henry's law, decreases as the temperature increases (Carroll et al, 1991). Indeed, Fig. 9 shows that as pressure and molar ratio increase, capture efficiency increases. Finally, according to the PCA (Fig 8), temperature and capture efficiency are orthogonal, there was no correlation between them.

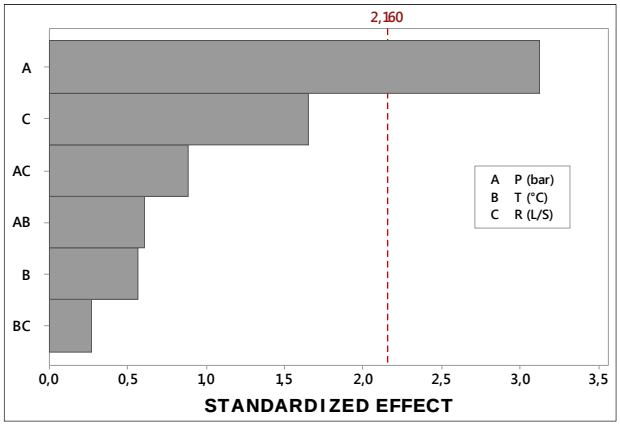

Fig. 5. Pareto diagram for experiments, (α =

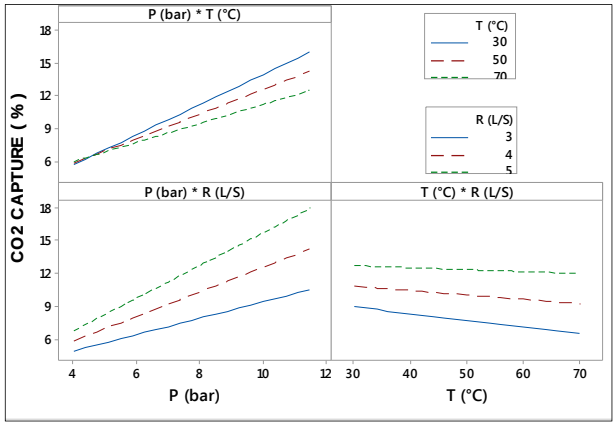

Fig. 6. Interactions diagram for experimental

0,05),

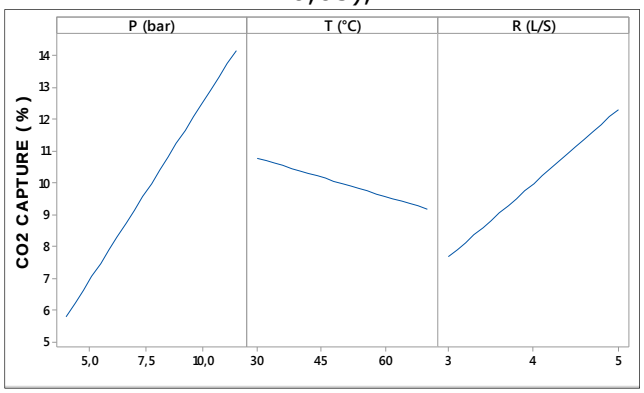

Fig. 7. Influence of experimental variables on efficiency based on the initial content of CKD

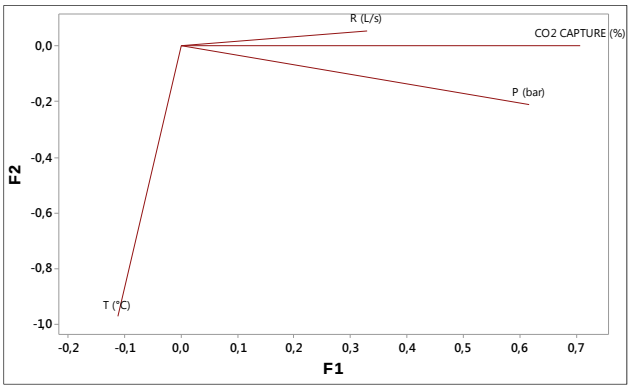

Fig. 8 Principal components analysis –PCA for experimental variables

variables on CO_2 capture potential

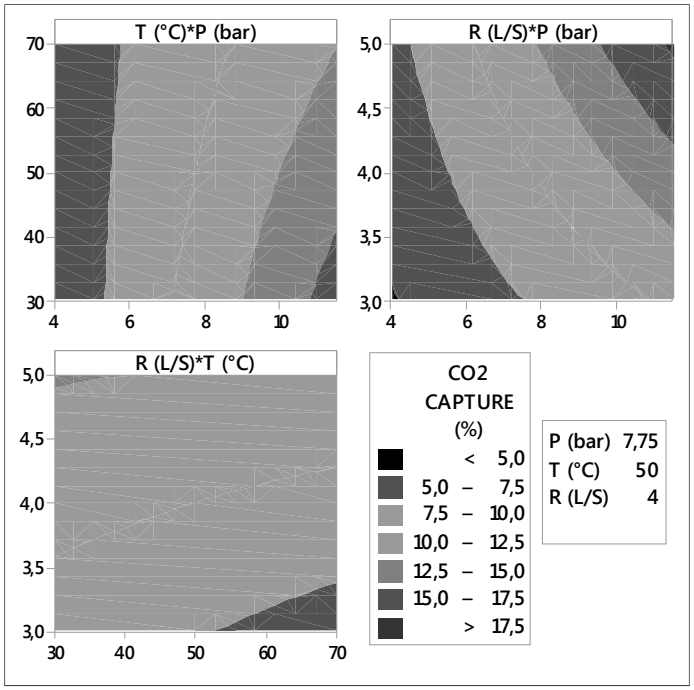

Fig. 9. Contour diagrams for influence of experimental variables on efficiency based on the initial content of CKD

3.3 Characterization of materials produced by carbonation

Thermogravimetric analysis

Table 2 illustrates percentage of mass loss when a sample is heated up to 900 ºC. This is a measure of amount of carbonates liberated as gaseous CO_2, as in equation 8. Net loss is calculated from TGA for results CKD. Sample 3 did not capture CO_2 effectively; mass loss of the product was lower than CKD. CO_2 capture uptake was less 0.5%.

Table 2. TG Analysis results for post carbonated products, T_i is the initial temperature for decarbonation; T_{max} is the maximum temperature for decarbonation; Δm is the total mass loss due to decarbonation.

No.	T_i (°C)	T_{max} (°C)	Δm (%)	Net Loss	No.	T_i (°C)	T_{max} (°C)	Δm (%)	Net Loss	Chemical transformation
CKD	474.0	745.5	35.13	-	10	470.8	741.2	36.69	1.56	
1	495.5	741.2	34.84	0.00	11	323.5	741.2	37.02	1.89	
2	302.0	741.2	35.88	0.75	12	409.5	741.2	35.92	0.79	
3	495.5	736.9	34.84	0.00	13	366.5	741.2	36.05	0.92	
4	302.0	741.2	35.89	0.76	15	366.5	741.2	36.50	1.37	$CaCO_3 \rightarrow CaO + CO_2 \uparrow$ (8)
5	474.0	741.2	35.37	0.24	16	388.0	754.1	36.36	1.22	
6	409.5	745.5	36.46	1.33	17	409.5	792.8	36.34	1.21	
7	452.5	745.5	37.56	2.43	18	452.5	745.4	37.03	1.90	
8	388.0	741.2	36.37	1.24	19	431.0	745.5	36.69	1.56	
9	366.0	745.5	35.55	0.42	20	431.0	741.2	36.50	1.37	

Analysis of functional groups, FT-IR

Functional groups were determined by FT-IR. In all samples, carbonates were found at 1430 cm^{-1} and 877 cm^{-1}. As **Fig 10** shows, $CaCO_3$ and $MgCO_3$ are in the same band. Some differences can be identified using XRD and SEM analysis (Miller & Wilkins, 1952)(Velts et al, 2014). Water is a key factor to activated carbonation (Montes-Hernandez et al., 2010). In Fig. 10, those experiments with high molar ratio (L/S) have intensive bands. Although temperature can affect, it influence is lower than liquid relation.

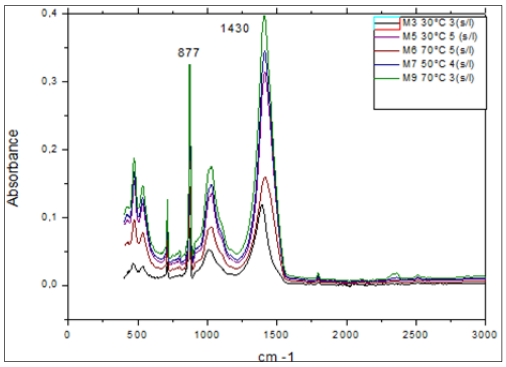

10-a Carbonated obtained at 4 bar

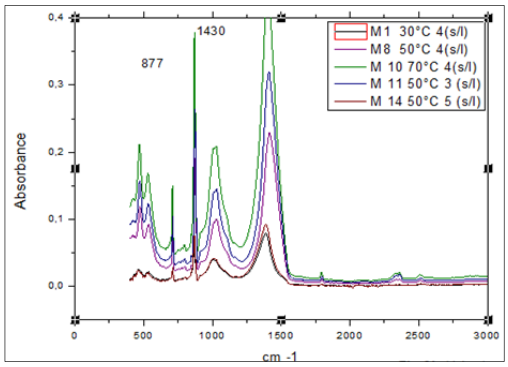

10-b Carbonated obtained at 8 bar.

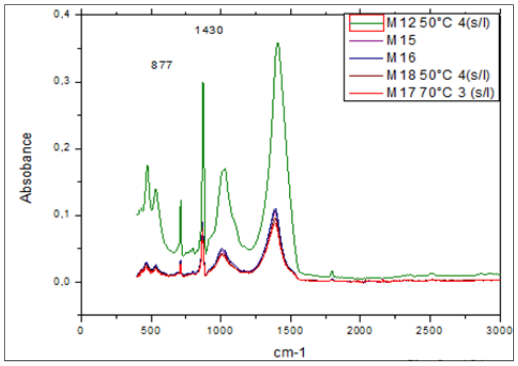

10-c Carbonated obtained at 12 bar.

Fig. 10. FTIR Analysis for post carbonated products.

Morphological Analysis (XDR and SEM)

According to SEM, the rhombic form is present, which is a calcite polymorphous in environment condition (Mayoral et al, 2013) (Ben Ghacham et al, 2015). Figure 11-c presents that as pressure increases morphology improve. Figure 11-a, show how sample is scattered.

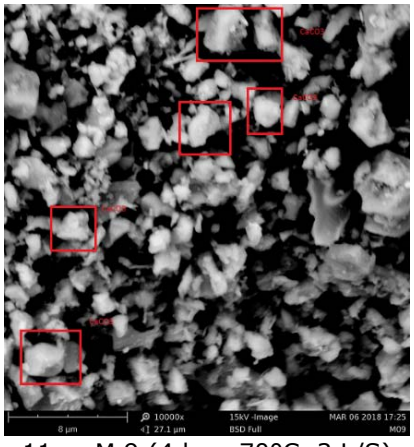

11-a. M 9 (4 bar, 70ºC, 3 L/S)

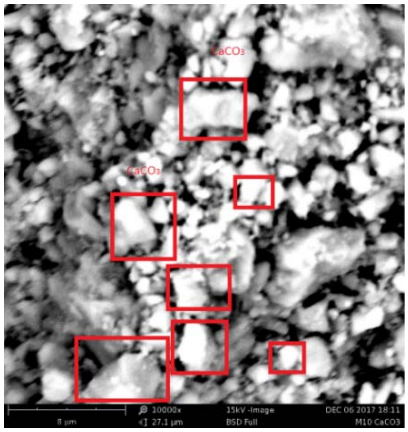

11-b. M 10 (8 bar, 70ºC, 4 L/S),

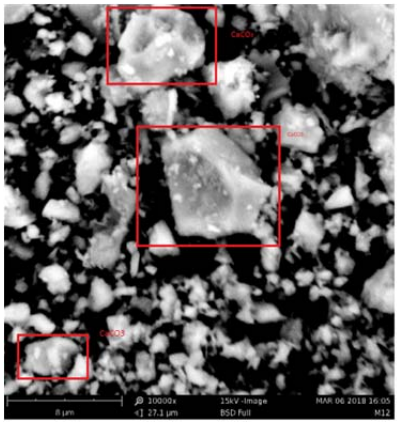

11-c. M 12 (12 bar,50ºC,4 L/S)

Fig. 11. SEM images for post carbonated products (10000x)

The XRD spectra for $CaCO_3$ precipitate shows characteristic peaks in 23.01°, 29.3°, and 43.66°, (Chang et al, 2011)(Azdarpour et al., 2014). Instead, spectra for post-carbonated samples (Fig 12a-c), show the main peaks between 29° and 30°, which corresponds to $CaCO_3$ (Sun et al., 2012). Other phases were found to include $MgCO_3$ and SiO_2 but in lower quantities. *Rielveld refinement* included a background, Wyckoff placements, group R-3c for calcite, and the pseudo-voight function for adjusting peak shape. *Rielveld refinement* (Fig 12-d) showed that pressure is an important factor to form calcite precipitate, and that 50% of the product corresponds to $CaCO_3$, and 10% to SiO_2.

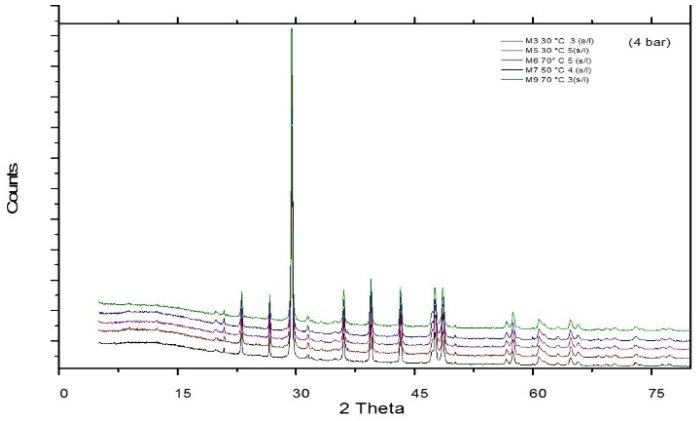

12-a Products carbonated obtained at 4 bar

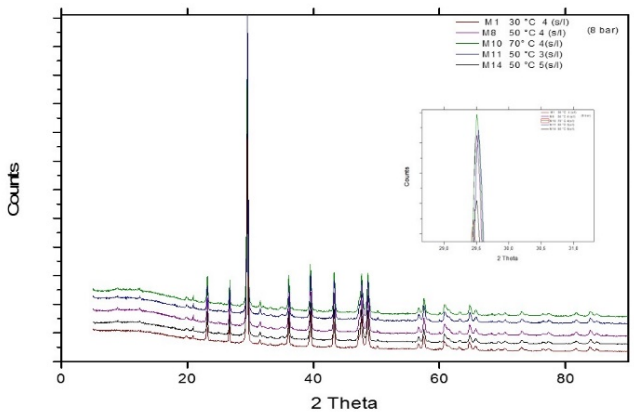

12-b Products carbonated obtained at 8 bar.

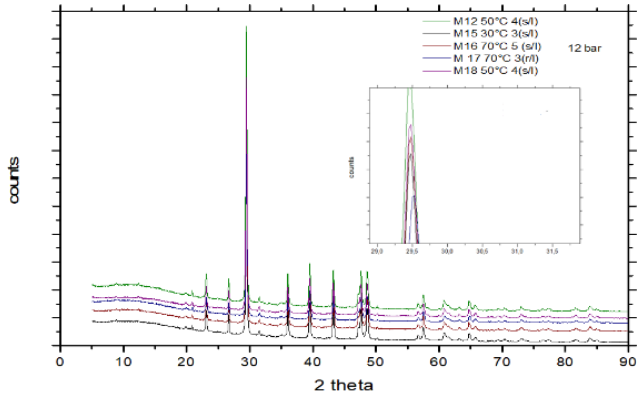

12-c Products carbonated obtained at 12 bar.

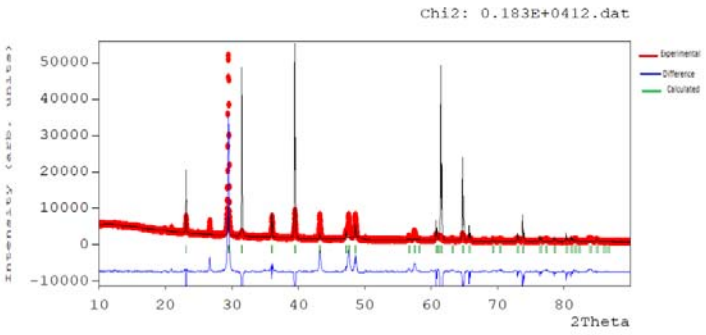

11-d Reilvet refinement for M12

Fig. 12. XRD diffractogram for post carbonated products.

Particle Size distribution

In general, post-carbonated products have similar size distributions (Fig. 13), more than 30% being among 3-13 µm. The carbonate ion diffuses into the solid resulting in a growing front of carbonated material surrounding an internal zone of non-carbonated material (Fernández Bertos et al., 2004), (Sanna, 2015).

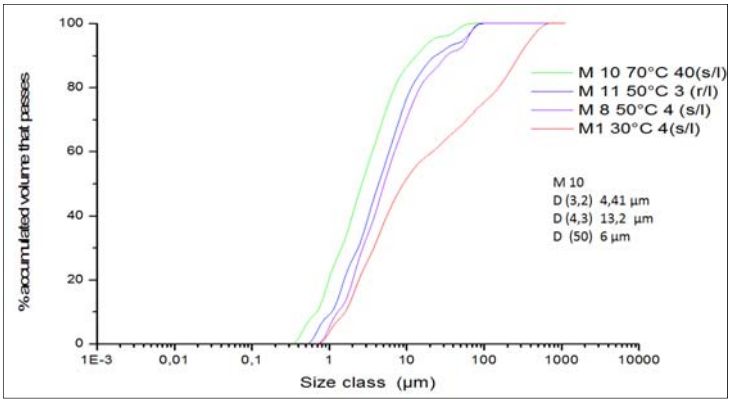

13-a Carbonated obtained at 4 bar

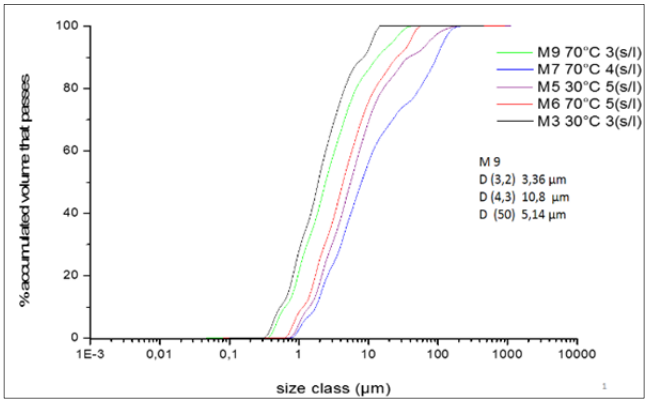

13-b Carbonated obtained at 8 bar.

Fig. 13. Particle size distribution for post carbonated products

4. Conclusions

Our results showed that CO_2 capture does not depend highly on temperature and molar ratio. The main variable influence on capture uptake is pressure, which defines the amount of CO_2 in the system according to the real gas law and the Redlich-Kwong model. Indeed, according to the PCA results, there was no correlation between temperature and capture uptake. In addition, the variables temperature and ratio molar, and its interactions such as temperature-ratio molar, pressure-temperature, and pressure-ratio molar, which do not exceed the statistical limit of the p-value, represent a negligible contribution. Interaction between variables pressure-temperature-ratio molar was evaluated, as a result, the favorable conditions of the capture system they are given at a high pressure and ratio molar, and it is the operating conditions that must be established.

Furthermore, pressure, and ratio molar liquid-solid have a great influence over physical properties of materials obtained. In a structural level, pressure have a high influence on $CaCO_3$ formation: the experiment at 8 and 12 bar have a great percentage of calcite, although SiO_2 and $MgCaCO_3$, were also present in products. $MgCaCO_3$ was formed because initial magnesium content in CKD was 0.61% w.t. Infrared spectroscopy show us intensive bands at higher water contents. Water is a key factor, because it allows calcium and magnesium ions to be transported into aqueous phase. Finally, particle size of products was 3-13 μm, optimum for some industrial applications.

5. Acknowledgements

Authors are grateful to Dirección de Investigación y Extensión de Sede Bogota at Universidad Nacional de Colombia, and to Vicerrectoría de Investigación of Universidad ECCI as co-funding entities of the research. We greatly appreciate Professor Ignacio Rodriguez for his invaluable contributions to build and run the reactor for our experiments.

6. References

Ahmari, S., & Zhang, L. (2013). Utilization of cement kiln dust (CKD) to enhance mine tailings-based geopolymer bricks. *Construction and Building Materials*, *40*, 1002–1011. http://doi.org/10.1016/j.conbuildmat.2012.11.069

Azdarpour, A., Asadullah, M., Junin, R., Manan, M., Hamidi, H., & Mohammadian, E. (2014). Direct carbonation of red gypsum to produce solid carbonates. *Fuel Processing Technology*, *126*, 429–434. http://doi.org/10.1016/j.fuproc.2014.05.028

Bernal, B. A. F., & Saavedra, K. A. H. (2008). *DIAGNÓSTICO DE LA INDUSTRIA DEL CEMENTO EN COLOMBIA Y EVALUACIÓN DE ALTERNATIVAS TECNOLÓGICAS PARA EL CUMPLIMENTO DE LA NORMA DE EMISIÓN DE FUENTES FIJAS*. *Journal of Chemical Information and Modeling*. Universidad de la Salle.

Bobicki, E. R., Liu, Q., Xu, Z., & Zeng, H. (2012). Carbon capture and storage using alkaline industrial wastes. *Progress in Energy and Combustion Science*, *38*(2), 302–320. http://doi.org/10.1016/j.pecs.2011.11.002

Carroll, J. J., Slupsky, J. D., & Mather, A. E. (1991). The solubility of carbon dioxide in water. *Journal of Physical and Chemical*, *20*(6), 1201–1209. http://doi.org/10.1063/1.555900

Chang, E., Chen, C., Chen, Y., Pan, S., & Chiang, P. (2011). Performance evaluation for carbonation of steel-making slags in a slurry reactor, *186*, 2010–2011. http://doi.org/10.1016/j.jhazmat.2010.11.038

El-Naas, M. H., El Gamal, M., Hameedi, S., & Mohamed, A. M. O. (2015). CO2 sequestration using accelerated gas-solid carbonation of pre-treated EAF steel-making bag house dust. *Journal of Environmental Management*, *156*, 218–224. http://doi.org/10.1016/j.jenvman.2015.03.040

Fernández Bertos, M., Simons, S. J. R., Hills, C. D., & Carey, P. J. (2004). A review of accelerated carbonation technology in the treatment of cement-based materials and sequestration of CO2. *Journal of Hazardous Materials*, *112*(3), 193–205. http://doi.org/10.1016/j.jhazmat.2004.04.019

Gil Chaves, I. D., López, J. R. G., García Zapata, J. L., Leguizamón Robayo, A., & Rodríguez Niño, G.

(2016). Chapter 2 Thermodynamic and Property Models. In *Process Analysis and Simulation in Chemical Engineering*. http://doi.org/10.1007/978-3-319-14812-0

Huntzinger, D. N., Gierke, J. S., Sutter, L. L., Kawatra, S. K., & Eisele, T. C. (2009). Mineral carbonation for carbon sequestration in cement kiln dust from waste piles. *Journal of Hazardous Materials*, *168*(1), 31–37. http://doi.org/10.1016/j.jhazmat.2009.01.122

IDEAM. (2015). Inventario Nacional de Gases de Efecto Invernadero.

Kirchofer, A., Brandt, A., Krevor, S., & Prigiobbe, V. (2013). Assessing the Potential of Mineral Carbonation with Industrial Alkalinity Sources in the U . S . *Energy Procedia*, *37*, 5858–5869. http://doi.org/10.1016/j.egypro.2013.06.510

Kunal, P., Siddique, R., & Rajor, A. (2012). Use of cement kiln dust in cement concrete and its leachate characteristics. *Resources, Conservation and Recycling*, *61*, 59–68. http://doi.org/10.1016/j.resconrec.2012.01.006

Martínez, E. A., Tobón, J. I., & Morales, J. G. (2014). Coal acid mine drainage treatment using cement kiln dust. *Dyna*, *81*(186), 87. http://doi.org/10.15446/dyna.v81n186.38834

Maslehuddin, M., Al-Amoudi, O. S. B., Rahman, M. K., Ali, M. R., & Barry, M. S. (2009). Properties of cement kiln dust concrete. *Construction and Building Materials*, *23*(6), 2357–2361. http://doi.org/10.1016/j.conbuildmat.2008.11.002

Miller, F. A., & Wilkins, C. H. (1952). Infrared Spectra and Characteristic Frequencies of Inorganic Ions. *Analytical Chemistry*, *24*(8), 1253–1294. http://doi.org/10.1021/ac60068a007

Montes-Hernandez, G., Pommerol, A., Renard, F., Beck, P., Quirico, E., & Brissaud, O. (2010). In situ kinetic measurements of gas-solid carbonation of Ca(OH)2 by using an infrared microscope coupled to a reaction cell. *Chemical Engineering Journal*, *161*(1–2), 250–256. http://doi.org/10.1016/j.cej.2010.04.041

Sanna, A. (2015). Reduction of CO2 Emissions Through Waste Materials Recycling by Mineral Carbonation. *Handbook of Clean Energy Systems*. http://doi.org/10.1002/9781118991978.hces025

Sreekrishnavilasam, A., King, S., & Santagata, M. (2006). Characterization of fresh and landfilled cement kiln dust for reuse in construction applications. *Engineering Geology*, *85*(1–2), 165–173. http://doi.org/10.1016/j.enggeo.2005.09.036

Styring, P., Quadrelli, E., & Armstrong, K. (2014). *Carbon Dioxide Utilisation: Closing the Carbon Cycle*. http://doi.org/978-0-444-62746-9

Sun, Y., Parikh, V., & Zhang, L. (2012). Sequestration of carbon dioxide by indirect mineralization using Victorian brown coal fly ash. *Journal of Hazardous Materials*, *209–210*, 458–466. http://doi.org/10.1016/j.jhazmat.2012.01.053

Ukwattage, N. L., Ranjith, P. G., & Li, X. (2017). Steel-making slag for mineral sequestration of carbon dioxide by accelerated carbonation. *Measurement: Journal of the International Measurement Confederation*, *97*, 15–22. http://doi.org/10.1016/j.measurement.2016.10.057

Velts, O., Kindsigo, M., Uibu, M., Kallas, J., & Kuusik, R. (2014). CO2 mineralisation: Production of CaCO3-type material in a continuous flow disintegrator-reactor. *Energy Procedia*, *63*, 5904–5911. http://doi.org/10.1016/j.egypro.2014.11.625

Yuen, Y. T., Sharratt, P. N., & Jie, B. (2016). Carbon dioxide mineralization process design and evaluation: concepts, case studies, and considerations. *Environmental Science and Pollution Research*, *23*(22), 22309–22330. http://doi.org/10.1007/s11356-016-6512-9